J. Quant. Spectrosc. Radiat. Transfer. Vol. 9, pp. 31–47. Pergamon Press 1969. Printed in Great Britain

DISPERSION STUDIES OF THE 22 GHz WATER VAPOR LINE SHAPE

I. THE LORENTZIAN BEHAVIOR

H. J. LIEBE, M. C. THOMPSON, JR. and T. A. DILLON*

Environmental Science Services Administration Institute for Telecommunication Sciences, Tropospheric Telecommunications Laboratory, Boulder, Colorado 80302

(*Received* 19 *June* 1968)

Abstract—The line shape of the self-broadened rotational ($5_{-1} \rightarrow 6_{-5}$) transition of water vapor at $\nu_0 = 22.235$ GHz has been investigated on the basis of resonance dispersion information. Detailed information on absolute intensity, width, shift, and wing response was obtained without molecular effect modulation. A differential refractometer with one dual-mode cavity sensor was operated in the pressure range 5×10^{-4} to 20 torr at 27°C. The dispersion was measured at fixed frequencies ($\nu_0 \pm 250$ MHz) with slowly varying vapor pressure. In this first part of the study the results obtained for pressures above 0.1 torr are presented. For pressures higher than 2 torr, a Lorentzian line shape was confirmed with a constant maximum dispersion of $\pm 0.387 \times 10^{-6}$. Down to 0.1 torr, the line center displayed Lorentzian behavior with the pressure-linear width of 17.99 MHz/torr and a violet shift of 1.38 MHz/torr, but the wing dispersion dropped more rapidly with decreasing pressure while the maximum dispersion increased. The Lorentzian line strength was determined and found to be in good agreement with the theoretical value as determined by the transition probability for the asymmetric rotor. The experimental strength yielded a maximum linear power absorption coefficient of 7.21×10^{-6} cm^{-1}.

1. INTRODUCTION

MICROWAVE spectroscopy of gases has been an extremely useful tool for studying molecular properties, but an important portion of the spectroscopic information has remained unavailable: the absolute intensity and the detailed shape of a spectral line. Quantitative results are vital for supporting theories of molecular structure and interaction and for verifying one of the numerous models about pressure effects on line profiles. Data in the wing regions and studies of the pressure dependence of line parameters are particularly interesting.

The dispersion of the self-broadened rotational water vapor line (J_τ:$5_{-1} \rightarrow 6_{-5}$) at the transition frequency $\nu_0 = 22.235$ GHz has been investigated over a wide range of pressures with a differential refractometer.[1] This paper is restricted to a discussion of the results that could be fitted to a Lorentzian shape function and pressure-linear behavior of the shape parameters, strength S, half-width γ, and pressure-induced ν_0-shift δ.

The advantages of refraction spectroscopy may be summarized as follows: (1) the resonance dispersion approaches the asymptotic wing values of the frequency distribution more slowly, when compared with the absorption response, thereby supplying structural

* During the period of this research, Mr. Dillon was also doing theoretical work on line shapes at the University of Colorado, supported by the N.I.H. grant No. GM11123.

details in the wing regions; (2) the measurement is confined to one frequency (easy to stabilize), which allows the vapor pressure (difficult to stabilize in an enclosure) to be the experimental variable; (3) the dispersion signal changes sign at ν_0, resulting in a well-defined baseline; (4) for a Lorentzian shape, the maximum dispersion coincides with the half-power point, making this method particularly suitable for linewidth studies; (5) the signal can be calibrated in absolute terms to better than 10^{-8} as a frequency change. In an absorption experiment, a difference in power levels of the order of 10^{-8} is impossible to detect without molecular effect modulation (Stark, Zeeman, saturation effects), which destroys the equilibrium conditions and hence the "true" shape.

Although refraction spectroscopy has become an established procedure in infrared spectroscopy,[2] it has not been applied in the microwave region. The only exception is a paper dealing with the strong 3–3 inversion line of NH_3.[3] Our apparatus is a modified version of the two-cavity refractometer.[3–5] A dual-mode cavity resonator is used to translate the resonance dispersion into a measurable phase change,[6] increasing the reliability and resolution considerably.

The contribution of the rotational spectrum to the refractive index of atmospheric water vapor has been calculated by ZHEVAKIN and NAUMOV.[7] In reviewing experimental spectroscopy on rotational water vapor lines, we did not consider measurements in the free atmosphere (uncertain gas conditions). Experimental information about the 22 GHz line in pure water vapor has been limited to transition frequency and linewidth data.[8–10] Line shape results (10 per cent error) were obtained for moist air by BECKER and AUTLER.[11] Spectroscopy on the only other microwave water vapor line at $\nu_0 = 183.31$ GHz (82 times stronger), yielded linewidth information,[12] and irregularities in the far wings.[13] In the infrared, the linewidth and the absolute strength were measured for three fairly isolated H_2O lines, but were found to be in poor agreement with theoretical values.[14]

The experimental width results can be compared with the predictions by BENEDICT and KAPLAN,[15] and the theoretical line strengths can be calculated by using tables for the asymmetric rotor strengths.[16,17]

2. MICROWAVE REFRACTION SPECTROSCOPY

2.1. *Theory*

The interaction between a gas and electromagnetic radiation of frequency ν can be described by a complex refractive index

$$n^* = n'(\nu) - i \cdot n''(\nu), \tag{1}$$

where

$n'(\nu)$ is the refraction spectrum, and

$n''(\nu)$ is the absorption spectrum.

Both spectra are interrelated by Kramers–Kronig relations, a consequence of imposing the condition of strict causality on the interaction process.[18]

When the shape of an isolated spectral line is assumed to be Lorentzian in the vicinity of the molecular resonance, we can define

$$n'(\nu) = n'_0 - S \cdot \left(\frac{\Delta\nu + \delta}{(\Delta\nu + \delta)^2 + \gamma^2} \right) \text{ and} \tag{2}$$

$$n''(\nu) = S \cdot \left(\frac{\gamma}{(\Delta\nu + \delta)^2 + \gamma^2} \right). \tag{3}$$

The notations used are: S-line strength, γ-half-width of the line, δ-shift of the molecular resonance frequency ν_0, and $\Delta\nu = \nu - \nu_0$ (all $\Delta\nu \ll \nu$); n'_0 is the sum of the polarizabilities not associated with a spectral line and frequency-independent in the microwave region. A common expression for water vapor is[19]

$$n'_0 = 1 + \frac{p}{T}(A_1 + A_2/T) \cdot 10^{-6}. \tag{4}$$

The vapor pressure p is in torr; the temperature T in °K, and the constants are

$$A_1 = 95.46\,^\circ\text{K/torr and } A_2 = 499.5 \times 10^3\ ^\circ\text{K}^2\text{/torr}.$$

In the pressure range investigated (0.1 to 20 torr), all broadening mechanisms (wall, Doppler, saturation) except intermolecular collisions may be neglected. A Lorentzian shape is expected to represent the intensity distribution of a resolved collision-broadened line.[20] The strength, linewidth, and shift are assumed to be pressure proportional (binary collision model):

$$S = S^\circ \cdot p, \tag{5}$$

where the number of molecules is proportional to p, and

$$\gamma = \gamma^\circ \cdot p \tag{6}$$

$$\delta = \delta^\circ \cdot p, \tag{7}$$

where the collision rate is proportional to p. The superscript ° indicates per torr.

The line strength S° as defined by the Lorentzian function (equations (2), (5) and (19)) was calculated from the quantum mechanical equations for transition probabilities.[16] A general expression for asymmetric rotor molecules is

$$S^\circ = \frac{K}{T^{7/2}} \sqrt{(ABC)} \cdot g(I) \cdot \exp(-E_l/kT) \cdot S^x(\kappa) \cdot \mu_x^2 \cdot \nu_0, \tag{8}$$

where

$$K = \frac{1}{3} \sqrt{\left(\frac{\pi h^3}{k^7} \right)},$$

and h, k are Planck's and Boltzmann's constants. The water vapor transition investigated has the following spectroscopic parameters:

(a) $\nu_0 = 22.23515$ GHz, a value obtained from measurements at 10^{-3} torr (see Table 1);
(b) $A = 835.741$, $B = 435.064$, $C = 278.361$ GHz, the rotational constants;[21]
(c) $E_l = 13{,}402.14$ GHz, the energy of the lower state;[22]

(d) $\exp(-E_l/kT) = 0.11718$, the corresponding Boltzmann factor for $T = 300°K$;
(e) $g(I) = 3$, the nuclear spin weighting factor;
(f) The dipole component, μ_x, has to be along the b-principal axis of inertia ($x \equiv b$) but represents the total permanent dipole moment, since the only axis permitted by the symmetry of H_2O is the intermediate b-axis. The most reliable value, obtained by Stark-effect measurements, is $\mu_x \equiv \mu = 1.884$ debye;[23]
(g) The rigid rotor transition strength, S^b, is tabulated for the rotational quantum numbers of the transition $J(K_a, K_c): 5(2, 3) \rightarrow 6(1, 6)$ as a function of the asymmetry parameter κ in increments of 0.1.[16,17] A polynomial interpolation to the value for H_2O

$$\kappa = \frac{2B\text{-}A\text{-}C}{A\text{-}C} = -0.437715,$$ gave the result, $S^b(\kappa) = 0.055218$.

Substituting the H_2O parameters into equation (8) yields for $T = 300 \pm 1°K$

$$S^\circ = 14.329 \pm 0.047 \text{ Hz/torr}.$$

The linewidth parameter has been calculated as $\gamma^\circ = 19.5$ MHz/torr, on the assumption of solely dipole–dipole interactions by BENEDICT and KAPLAN.[15] A pressure-induced shift of the transition frequency is predicted[20,24] and has been observed for the 3–3 inversion line of NH_3 as a violet shift with the ratio of $\gamma^\circ/\delta^\circ = 56$.[25]

Except for a small shift term, all parameters have been determined theoretically defining the refraction (equation (2)) and the absorption (equation (3)) spectrum. In principle, it does not matter which one is chosen for an experimental check but we preferred the refraction spectrum because of the reasons summarized in Section 1.

2.2. *Experimental principle*

A differential measurement of the refractive index at two different frequencies, ν and ν_r, contains only the resonance dispersion

$$\Delta n = n'(\nu) - n'(\nu_r) = -S \cdot \left(\frac{\Delta\nu + \delta}{(\Delta\nu + \delta)^2 + \gamma^2} \right), \tag{10}$$

if the reference frequency ν_r is remote from the molecular resonance ($n'_0(\nu) = n'_0(\nu_r)$). We also assumed that the dispersion contribution of the wings of higher transitions of the rotational spectrum involved[22] is negligible (small linewidths) which has been verified for water vapor in the microwave region.[7]

A dual-mode transmission cavity as described by THOMPSON and VETTER[6] was found to be a very suitable detector for Δn. One mode resonates at $\nu_c \equiv \nu$, and the other mode has a perfect harmonic relationship,

$$\nu_r = \nu_c/m, \qquad m = \tfrac{1}{2}, \tfrac{1}{3}, \tfrac{1}{4}, \ldots \quad \text{or} \quad 2, 3, 4 \ldots. \tag{11}$$

The principles of measuring microwave refraction of gases with high Q cavities are well established. With various refinements, it is possible to resolve absolutely refractive index changes to better than 5 parts in 10^{-9}.[4,5]

The resonance ν_c of the evacuated cavity is set, determining

$$\Delta\nu \equiv \Delta\nu_c = \nu_c - \nu_0 = \text{const}. \tag{12}$$

The experimental variable is the pressure p. If we introduce water vapor into the cavity, the output of a differential refractometer records a pressure dispersion profile (equations (5), (6), (7), (10) and (12))

$$\Delta N(p) = \Delta n \cdot 10^6 = -S^\circ \cdot 10^6 \cdot p \cdot \left(\frac{\Delta \nu_c + \delta_c^\circ \cdot p}{(\Delta \nu_c + \delta_c^\circ \cdot p)^2 + (\gamma^\circ \cdot p)^2} \right). \tag{13}$$

The dispersion ΔN is measured in parts per million (ppm). The shift of the cavity vacuum resonance is δ_c°, which is the combined effect of a pressure-induced ν_0-shift δ^0, and the tuning of ν_c due to the pressure-proportional non-dispersive refractive index (equation (4)):

$$\delta_w^\circ = \nu_0 \left[\frac{A_1}{T} + \frac{A_2}{T^2} \right] 10^{-6} \equiv 0.126 \text{ MHz/torr at } T = 300^\circ\text{K}. \tag{14}$$

A comparison of a dispersion pressure profile with the more familiar frequency profile is shown in Fig. 1 for normalized scales. The distance along the frequency scale between the maximum and minimum dispersion is numerically equal to $2 \cdot \gamma$. The maximum dispersion, $\Delta N_{\max}$, occurs at the pressure

$$p_m = \Delta \nu_c / (\pm \gamma^\circ - \delta_c^\circ), \tag{15}$$

yielding (equation (13))

$$\Delta N_{\max} = \pm \frac{10^6 \cdot S^\circ}{2 \cdot \gamma^\circ},$$

and for the peak dispersion (Fig. 1)

$$\Delta N_0 = 2 \cdot |\Delta N_{\max}|. \tag{16}$$

The theoretical values of the strength and width predict a constant maximum dispersion signal of ± 0.37 ppm.

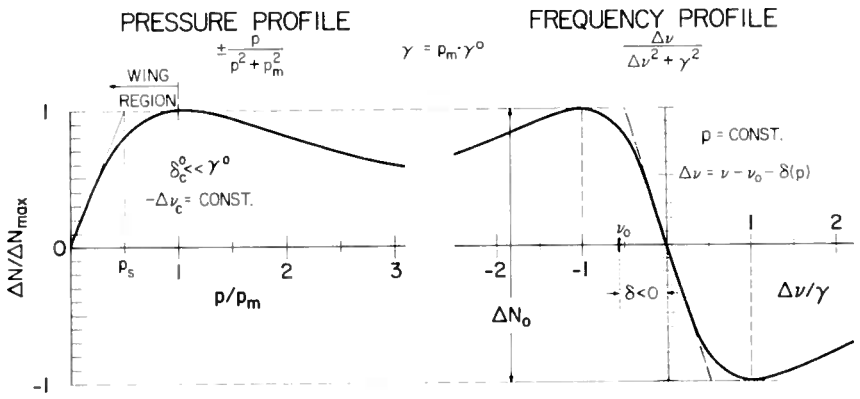

FIG. 1. Normalized pressure and frequency dispersion profiles for a Lorentzian shape function ($\delta^\circ \to 0$ for the pressure profile).

Further information obtainable from a pressure profile is the starting slope (Fig. 1),

$$p_m/p_s = 2[1+\delta_c^\circ/(\pm\gamma^\circ-\delta_c^\circ)], \tag{17}$$

which contains the wing response of all lines with pressures smaller than about $p_m/5$.

The line center slope on the frequency scale is

$$s(p) = \frac{S^\circ}{(\gamma^\circ)^2 \cdot p}. \tag{18}$$

The properties of the Lorentzian (equations (13)–(18)) provide the criteria to be applied to a measured pressure profile.

The connection with conventional absorption spectroscopy is given by the linear power absorption coefficient $\alpha = 4\pi \cdot \nu \cdot n''(\nu)/c$, which yields at ν_0 (equations (3), (5), and (6))

$$\alpha_0 = \frac{4\pi \cdot \nu_0 \cdot S^\circ}{c \cdot \gamma^0}. \tag{19}$$

3. EXPERIMENTAL TECHNIQUE

3.1. *Apparatus*

Technical details pertaining to the microwave dispersometer and its operation as a quantitative spectrometer will be discussed in Ref. 1. A few points bear mentioning, however. The schematic of the apparatus for the water vapor studies is shown in Fig. 2. The differential refractive index $\Delta N(p)$ is measured with a refractometer setup[4] having one

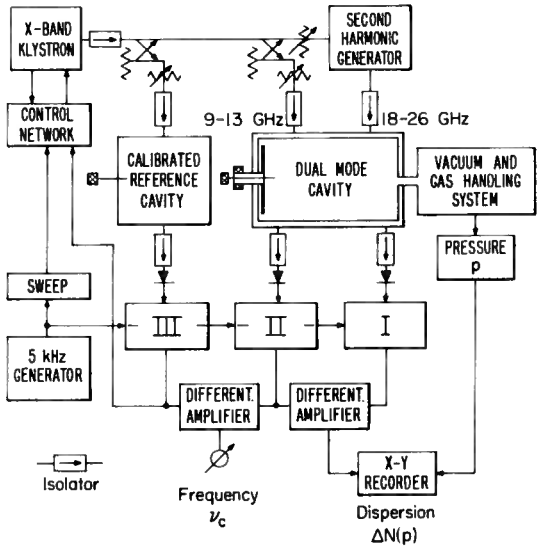

FIG. 2. Schematic of the microwave dispersometer. I, II, III represent equivalent circuitry used to derive a phase signal as described in detail in Refs. 1 and 4.

dual-mode cavity. The operation is based on the fact that harmonically related resonance frequencies maintain that relationship exactly when the cavity is filled with a non-dispersive gas, but the differential tuning balance is disturbed when the refractive indices behave differently at the two frequencies.

The bimodal cylindrical cavity (length 2.6 ± 1, dia. 4.0 cm) resonated in the vicinity of 11 and 22 GHz, with the mode combination TE 011/TE 322. The 1:2.029 ratio of the resonances was corrected to the harmonic relationship $m = 2(\pm 1 \times 10^{-8})$ by a small center tuning stub that does not affect the TE 322 resonance (zero field position). The relative transmission responses were equal with loaded Q values of $Q_l = 1.25 \times 10^4$ and 10 per cent transmission. Cross-coupling and interference between the two modes were avoided. The temperature stability was 3×10^{-6}/°C, but the differential stability between the two modes was better than 10^{-8}/°C.

The lower mode was excited by an 11 GHz klystron modulated by a linear, periodic sweep (5 kHz repetition) of sufficient amplitude to cover the transmission band ($\cong 4$ MHz). Part of the klystron power was fed into a second harmonic generator exciting the higher frequency mode.

The pulse trains obtained at the detectors at the output ports of the bimodal cavity are treated in a phase meter with two identical channels, I and II. The principle of the phase meter operation is described in Ref. 4. Only a very small part (< 1 per cent) around the peak value of each cavity resonance response is used to derive a phase signal with reference to the 5 kHz generator (starting of the sweep) and corresponding to tuning of that mode. The detection scheme locks on to the peak value and is virtually unaffected by circuitry instabilities.

The frequency was measured by a reference cavity with highly resolved and calibrated tuning around $\nu_0/2$. Its frequency was tuned to coincide with the lower mode of the bimodal cavity. This was accomplished when a second phase meter (consisting of channel II and an identical channel III, connected to the reference) read zero phase difference. The reference was a sealed, temperature-compensated (3×10^{-8}/°C) cavity calibrated by the National Bureau of Standards with a tuning range $(\nu_0/2) \pm 7$ MHz. The resolution was on the order of 5×10^{-7}, but could be improved to 5×10^{-8} by temperature-tuning the dual-mode cavity and converting the temperature-time dependence to a frequency change (see Fig. 4). The frequency standard also served to keep the klystron center frequency at the cavity resonances. For measurements exceeding the tuning range, it was replaced by a commercial frequency meter with a resolution of 5×10^{-6}.

The water vapor was pumped off highly pure and gas-free water contained in a glass bulb. The pressure was controlled by an all-metal leak valve with a conductance variable from 10^2 to 10^{-10} cm^3/sec. A dual-stage rotary pump with an adsorption trap provided a minimum pressure of 1×10^{-5} torr in the system, which was checked for leaks with a He-leak detector. Controlling the water vapor was difficult. The concentration of the sample inside the cell changed because of adsorption and condensation on the walls.[5] The area-to-volume ratio was kept as small as possible by bringing the cell, valves, and the pressure sensor closely together and using large cross sections.

A capacitance manometer with two sensing heads from 10^{-3} to 10^2 torr monitored the true pressure. The absolute calibration in the lower ranges was accomplished with a McLeod gauge (1 per cent error) and in the higher ranges with a quartz Bourdon gauge (0.2 per cent error) using argon.

The resolving power of the differential refractometer, Q_R, was measured in the 10^{-3} to 10^{-2} torr pressure range and found to be larger than 125 000.[1] Effects of finite resolving power are a decrease in ΔN_0 and an increase in γ^0.[2] They are of no concern when

$$Q_R \gg Q_L = \frac{\nu_0}{2 \cdot \gamma^\circ \cdot p}. \tag{20}$$

The Q-value of the gas resonance, Q_L, at $p = 0.1$ torr is 6200. Thus the finite resolving power will have no influence on the experimental results.

As the cavity resonance frequency shifts under the influence of the gas, both the phase and the amplitude of the signal transmitted through the cavity vary. The change in the transmitted peak amplitude is determined by the ratio of the loaded cavity Q value to the interaction strength of the gas resonance, expressed by the medium Q value[26]

$$Q_m = \frac{\gamma^\circ}{S^\circ} \equiv 1.3 \times 10^6 \tag{21}$$

The phase detection is insensitive to the small changes in the amplitude of the transmitted cavity response.

The noise level of the detection was $\Delta N \approx 0.006$ ppm (with an averaging time constant of 0.1 sec at the output), equivalent to a minimum detectable absorption coefficient of $5 \times 10^{-8}\,\mathrm{cm}^{-1}$ (equations 16 and 19). The sensitivity (sweep amplitude) was adjusted to roughly ± 1 ppm/0.5 V (full Y-axis deflection) and calibrated for each "run" (see Section 3.2). The linear range of the phase detection was equivalent to a maximum output of ± 30 ppm, about twenty times larger than necessary.

3.2. *Procedure*

The following procedure was adopted to record dispersion pressure profiles of water vapor (equation (13)). First, the higher mode (TE 322) frequency ν_c was set at the desired deviation from the molecular resonance ν_0. The next step was to carefully adjust the lower mode (TE 011) frequency to a perfect harmonic ratio, $m = 2$. The cavity spectrometer cell was then pumped out for a considerable time (generally overnight) to remove adsorbed water vapor. The dispersometer was calibrated in absolute dispersion, ΔN (ppm) using the non-dispersive refractivity of dry argon. The phase change of either mode (I or II) with respect to the stable reference cavity (III) was measured in a two-cavity refractometer operation.[4,5] The argon pressure p_a corresponding to full Y scale (ΔN) deflection is converted to refractivity by[19]

$$N_a = 99.80 \cdot p_a\,(\mathrm{torr})/T(^\circ\mathrm{K}),\ \mathrm{ppm}. \tag{22}$$

A pressure "run" with argon provided a method of checking the differential stability, which depends, to first approximation upon how accurately $m = 2$ is tuned. Typically, for $p_a = 100$ torr ($N_a = 33.4$ ppm) the differential output indicated $|\Delta N_a| \leq 0.015$ ppm, which means that the differential stability was better than 1:2200. All experiments were conducted at a temperature of $27 \pm 1^\circ$C, where water vapor saturates at 26.7 ± 1.5 torr.

When water vapor was admitted slowly (10–30 sec/trace) to the cavity, one could either measure the total refractivity (equation (2)) at $\nu_c = \nu_0 + \Delta\nu_c$ and at $\nu_c/2$, or the dispersion

(equation (13)) between these two frequencies (Figs. 3 and 4). More than 20 refraction and 200 calibrated dispersion pressure profiles for $\Delta\nu_c = \pm 250$ MHz were taken, each over a pressure range 10^{-4} to 20 torr. At $\nu_c/2$ the validity of equation (4) was confirmed.

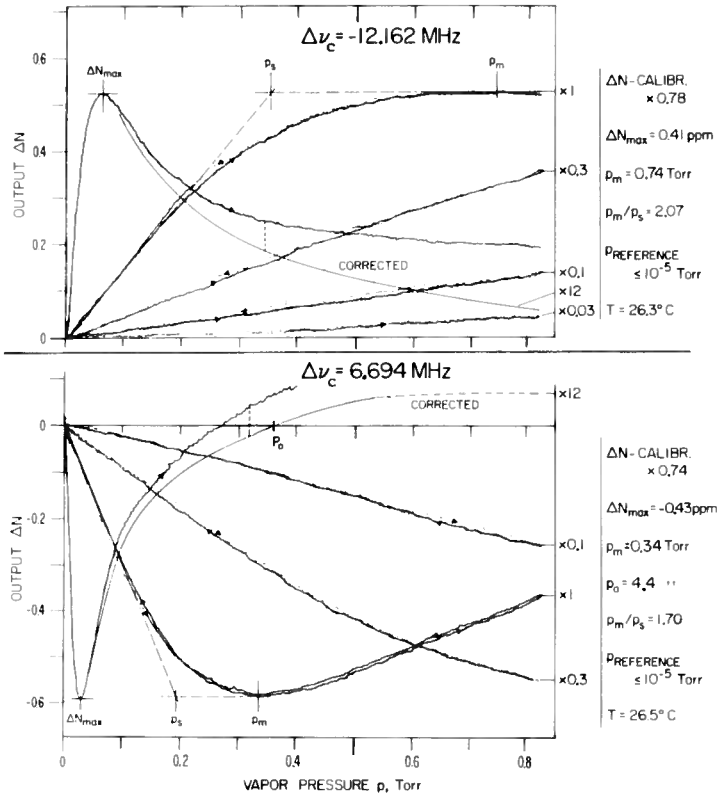

FIG. 3. Two original X/Y plots of pressure profiles, with the definition of the experimental parameters and a listing of the actual values. The scale factors on the right side refer to the pressure scale.

During the 10-month period of the measurements, particular care was taken to check consistency. The data were recorded with increasing and decreasing pressure. Up to 1 torr, there was no noticeable hysteresis effect (Fig. 3). The same trace was followed even when the pressure decreased by wall adsorption, which was as high as 65 per cent in the 0.1 torr range for a clean cavity. A series of test measurements were performed and excellent reproducibility was found under different conditions (microwave power level at ν_c, phase meter balancing, forward and backward sweep, clipping level). The only severe effect was the positive biasing of the data beyond 1 torr pressure. This pressure-linear effect was caused by heavy condensation on the cavity walls and the high non-dispersive refractivity (for $p = 10$ torr it follows from equation (4) that $(n'_0 - 1) = 56.5$ ppm), both disturbing the

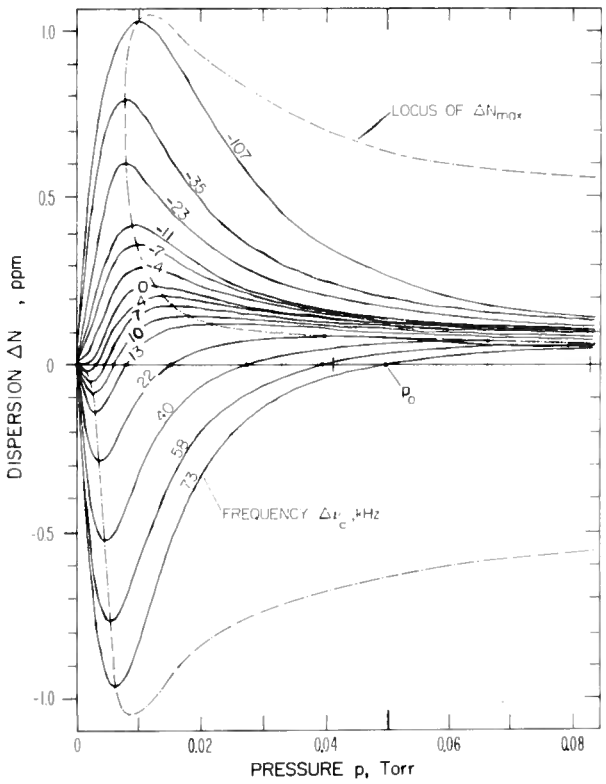

FIG. 4. Original X/Y plot of pressure profiles for temperature-tuning (-60 kHz/°C) through the line center. The rate of change was about 100 Hz/sec and each trace took 10 sec to record ($\Delta\nu_c$ = 73 kHz at 24.6°C, -107 kHz at 27.6°C); p_0 is listed in Table 1.

differential balance (equation (21)). The criterion for a correction was the symmetry of ΔN_{max} to the baseline in respect to $\pm\Delta\nu_c$. The amount of correction was on the order of

$$\Delta N_b = (0.01 \pm 0.005) \cdot p\,(\text{torr}),\ \text{ppm} \tag{23}$$

which was cross-checked by the coordinate of p_0 (Table 1).

4. RESULTS

The microwave dispersion spectrometer has the sensitivity and resolving power to make accurate measurements of the shape, width, and shift of the water vapor line. A simple method of line parameter measurements emerges from the Lorentzian shape function. Our objectives were to examine the validity of equation (2) using pressure profiles (equation (13)) over a wide range of vapor pressures at room temperature and to determine the two molecular ($\nu_0, S°$) and the two interaction ($\gamma°, \delta°$) parameters.

The microwave power level at the cavity input port (20 μW at ν_c) was sufficiently low so that power saturation was avoided down to at least 10^{-2} torr. The linewidth caused by wall collisions was calculated to be 8 kHz, which is negligible, as is the Doppler width of 33 kHz.

4.1. *Maximum dispersion*

After analyzing the pressure profiles (Figs. 3 and 4), we plotted the envelope of the maximum dispersion versus the frequency setting as shown in Fig. 5. These absolute

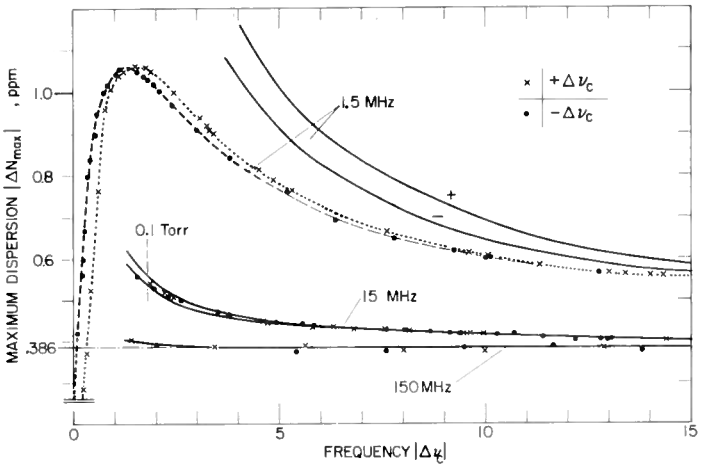

FIG. 5. The maximum dispersion $|\Delta N_{max}(p)|$ as a function of the frequency setting, $\Delta\nu_c$. The solid lines are calculated with equation (25).

intensity data proved to be the most reliable of all the data. The calibration according to equation (22) was accomplished with an accuracy of better than ± 0.01 ppm. The asymptotic value of $\Delta N_{max} = \pm 0.39$ ppm, approached for $|\Delta\nu_c| \geq 35$ MHz and $p \geq 2$ torr is in close agreement with the theoretical values (equation (16)). The increase of ΔN_{max} closer to the line center was the first indication that the shape function and/or the line parameters were changing with decreasing pressure.

4.2. *Data analysis*

A straightforward and most critical test of the shape function consisted of the following procedure. A large number of data points (about 3000) taken from pressure profiles at 55 frequencies ($\nu_0 \pm 14$ MHz) were fitted to a Lorentzian (equation (10)), using the method of least squares. The parameters S, γ, and δ were calculated for 40 values of pressure between 10^{-3} and 1 torr, and a nonlinear pressure dependence for all three was obtained. A Lorentzian line shape could not account for the detailed experimental data and the inclusion of the Doppler effect and finite resolving power* based on the Voigt profile shape function did not improve the results.

* The finite linewidth to be resolved was 90 kHz as compared with the Doppler width of 33 kHz.

In a less comprehensive, more conventional analysis we used the relationship between the frequency setting $\Delta\nu_c$ and the pressure coordinate p_m of the maximum dispersion. The coordinates of the dispersion maxima in the pressure range $p_m + 47$ to 840 mtorr* (96 points) could be fitted to equation (15). A least square computer program determined the slope of each $\Delta\nu_c$ branch and all pertinent error information. The result is for

$$\begin{aligned} +\Delta\nu : \gamma^\circ - \delta_c^\circ &= 19.50 \text{ MHz/torr, and for} \\ -\Delta\nu : \gamma^\circ + \delta_c^\circ &= -16.48 \text{ MHz/torr.} \end{aligned} \tag{24}$$

The RMS-deviation from the fitted straight line was 0.015 MHz. Experimental points are plotted in Fig. 6. There is no doubt that the locus of the maximum dispersion (assumed to be representative of the linewidth) varies exactly as the first power of pressure between 0.1 and 1 torr. From the constant maximum dispersion (Fig. 5), the pressure range can be extended to about 13 torr with less certainty, because of the mistuning corrections (equation (23)).

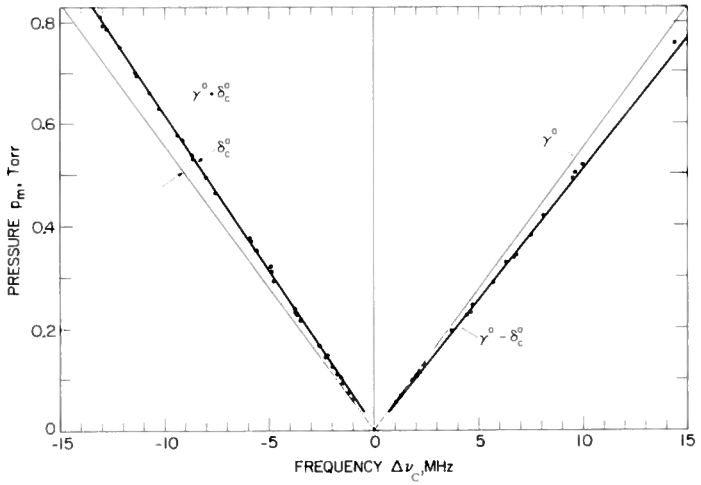

FIG. 6. The pressure-linear (Lorentzian) relationship between the frequency setting, $\Delta\nu_c$ and the pressure coordinate at maximum dispersion, p_m.

4.3. *Transition frequency*

The transition frequency was defined by the first pressure profile that did not show a zero-crossing when the decreasing frequency ν_c slowly passed over the line center (Fig. 4). The frequency at $p = 1$ mtorr was found to be $\nu_0 = 22{,}235.15 \pm 0.01$ MHz (Table 2).

4.4. *Shift*

An apparent shift of ν_0 to higher frequencies of $\delta_c^\circ = -1.51$ MHz/torr follows from equation (24) and was confirmed by the independent information of zero-crossings (p_0) of the pressure profiles for the ($+\Delta\nu$)-part (Figs. 3 and 4). The average of these results, which are listed in Table 1, agrees well with the value obtained from the locus of the maximum

* The upper limit was determined by the tuning limits of the highly stable frequency reference.

dispersion. The true line-shift parameter, δ°, is found by correcting for the refractive tuning (equation (14)) to

$$\delta^\circ = \delta_c^\circ - \delta_w^\circ = -1.38 \text{ MHz/torr (violet shift).}$$

TABLE 1. PRESSURE SHIFTS OBTAINED FROM ZERO-CROSSINGS OF $\Delta N(p)$

$+\Delta\nu_c \equiv -\delta_c$	p_0	$\delta_c^\circ = \delta_c/p_0$
(kHz)	(mtorr)	(MHz/torr)
0	0	0
4	2.5	−1.6
7	4.5	−1.55
10	6.5	−1.54
13	8.5	−1.53
22	15	−1.46
40	27	−1.48
58	39	−1.49
73	50	−1.46
(MHz)	(torr)	
0.342	0.23	−1.49
1.304	0.85	−1.54
5.773	*3.8	−1.52
6.694	*4.4	−1.52
9.404	*6.1	−1.54
		−1.515 ± 0.08

* Corrected for mistuning (equation (23)).

TABLE 2. HALF-WIDTH PARAMETERS FOR SELF-BROADENED WATER VAPOR LINES

Transition $J_\tau \to J'_{\tau'}$	Transition frequency ν_0	Vapor pressure p	Line width γ°	Method*	Temperature T	Reference
	MHz	torr	MHz/torr		°C	
$5_{-1} \to 6_{-5}$	22 320 ± 150	1–55 (+ Air)	16.1–19.1	A	45 ± 1	11
	22 237 ± 5	0.103	14.1 ± 2%	A	45	8
	22 235.17	0.029–0.209	16.5 ± 5%	S	≈ 24	9
	22 235	0.04	18.5	E	≈ 24	10
	22 235		19.5	Th	27	15
	22 235.15 ± 0.01 (at 1 *m*torr)	0.1–20	17.99 ± 1%	D	27 ± 1	This work
$2_2 \to 3_{-2}$	183 310.12 ± 0.1	0.04–0.12	19.06 ± 1%	A	27	12
	183 310	0.05–2	23 ± 9%	A	27	13
	183 310		18.7	Th	27	15

* A—Absorption spectrum; S—Power-saturated absorption spectrum; E—Emission spectrum; D—Dispersion spectrum; Th—Theoretical calculation by Anderson's Theory.

4.5. *Width*

Equation (26) yields a linewidth parameter of $\gamma^\circ = 17.99$ MHz/torr. A synopsis of the linewidth parameters reported for two rotational H_2O lines is given in Table 2, where the width value of the 22 GHz line has been determined by four different experimental methods. Comparison of these data with the theoretical values[15] leads us to agree with RUSK's[12]

comments on the unreliability of previous absorption measurements. The "dispersion"-width parameter is still 8.5 per cent lower than theory predicts, a discrepancy about five times that for the 183 GHz line, although both experiments claim a 1 per cent reliability. For strong dipole–dipole interactions and low energy transitions (22 GHz), perturbation methods are not really appropriate. MIZUSHIMA[24] modified ANDERSON's[20] theory of collision-broadening for the microwave region, but results for the water vapor line are not yet available. An indication of the magnitude of the intermolecular interaction is the distinction between the effective collision diameter (13.6 Å) as determined by our width parameter, and the kinetic theory value (2.52 Å).[20] The application of dispersion techniques to very accurate studies of foreign gas broadening is the subject of a separate paper.[27]

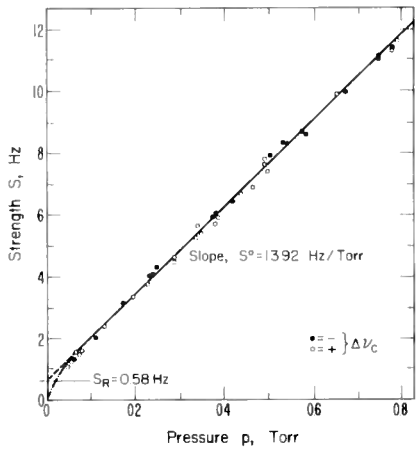

FIG. 7. The Lorentzian line strength plotted against pressure.

4.6. *Strength*

The advantages of refraction spectroscopy appeared clearly when we determined the absolute strength value. Once γ°, δ°, and ν_0 were determined, their values were substituted into the dispersion formula (equation (13)) and the strength as shown in Fig. 7 was calculated (least squares fit) for the experimental ΔN_{max}-values (Fig. 5). The strength, S, was found to be a linear function of pressure above 84 mtorr, with an RMS deviation of 0.035 Hz from the slope:

$$S^\circ = 13.92 \text{ Hz/torr}.$$

At zero pressure, however, the strength displays a positive intercept, $S_R = 0.58$ Hz. When this result with equation (15) is substituted into equation (10), we obtain

$$|\Delta N_{max}| = \frac{10^6}{2\gamma^\circ}\left[S^\circ + S_R \cdot \left(\frac{\pm\gamma^\circ - \delta_c^\circ}{\Delta\nu_c}\right)\right]. \tag{25}$$

This formula gives the solid lines shown in Fig. 5. The residual strength provides further evidence of anomalies below 0.1 torr.

The agreement between the experimental strength parameter and the value obtained from equation (8) is good ($S_x^\circ/S_{Th}^\circ = 0.972$), contrary to the results obtained for much stronger infrared lines.[14] The polynomial interpolation of the transition strength used for this calculation also gives the best agreement with recent Stark measurements.[23]

We might point out that the "residual" strength S_R merely collects the deviations from a pressure-linear Lorentzian shape. Applying CHAMBERLAINS's[28] method to our data at pressures 10^{-1} to 10^{-3} torr resulted in a pressure-linear integrated absorption strength which yielded an equivalent Lorentzian strength parameter, $S^\circ = 14.335$ Hz/torr. Whether the deviation from a Lorentzian line shape is due to a molecular effect or caused by the dispersometer will be investigated in Part II, to be published at a later date.

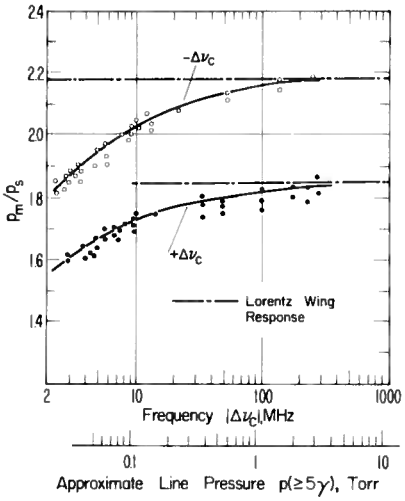

FIG. 8. The wing response, p_m/p_s.

4.7. *Wing response*

As previously stated, refraction spectroscopy provides reliable data on dispersion behavior in the wings of the molecular resonance. The criterion of equation (17) should be valid and yields the following values (equation (24)):

$$\begin{aligned} +\Delta\nu &: p_m/p_s = 1.845 \\ -\Delta\nu &: p_m/p_s = 2.183. \end{aligned} \tag{26}$$

As Fig. 8 shows, with decreasing pressure the dispersion in the wings becomes smaller than the corresponding Lorentzian value. The intensity distribution of the lines shows enhancement at the line center. The pressure range of the departure from the Lorentzian prediction agrees with the occurrence of anomalies in the maximum dispersion envelope (Fig. 5). The scattering of the data is caused by the graphical determination of the ratio, p_m/p_s (Fig. 3).

4.8. *Center slope*

The center slopes of five frequency profiles (0.1/0.2/0.5/1/2 torr) plotted on the basis of the experimental data were compared with equation (18). The value of the slope parameter

was graphically determined as 0.044 torr ppm/MHz (Table 3), further demonstrating the consistency of the "dispersion" strength and width.

4.9. *Summary*

The experimental results are summarized in Table 3. The peak dispersion ΔN_0 (equation (16)) and the absorption coefficient α_0 (equation (19)), were calculated from the experimental parameters. The four Lorentzian parameters were obtained from a large number of reliable and reproducible data points. These parameters represent the pure collision-broadening contribution, but they will not reproduce the dispersion profiles measured in any pressure

TABLE 3. EXPERIMENTAL LORENTZIAN 22 GHz H_2O LINE PARAMETERS AT 27°C

Parameter	Pressure dependence	Symbol	Value	Uncertainty	Units
(I) Valid in the pressure range 2–13 torr*					
Peak dispersion	None	ΔN_0	0.774	±0.015§	ppm
Line strength	None	S°	13.92	±2%§ 0.035‡	Hz/torr
Linear power absorption coefficient	None	α_0	7.212×10^{-6}	±2%§	cm^{-1}
Wing response	None	p_m/p_s at $-\Delta\nu$	2.18	±5%‖	1
		p_m/p_s at $+\Delta\nu$	1.85	±5%‖	1
(II) Valid in the pressure range 0.1–13 torr (Line Center)*					
Half-width	$\gamma = \gamma^\circ p$	γ°	17.99	±1%§ 0.015‡	MHz/torr
Pressure shift†	$\delta = \delta^\circ p$	δ°	−1.38	0.015‡	MHz/torr
Line center slope	$s = s_0/p$	s_0	0.044	±5%‖	torr ppm/MHz

* The highest pressure, p_m, where ΔN_{max} was measured was determined by tuning limitations ($\Delta\nu_c \leq 250$ MHz).
† Corrected for the refractive tuning (+0.126 MHz/torr).
‡ Standard deviation from pressure linearity.
§ Standard deviation (data scattering and calibration errors).
‖ Graphical solution.

region. However, the discrepancy decreases with increasing pressure above 0.1 torr, when a residual strength, S_R, is added to the pressure linear term, $S^\circ \cdot p$. Only above 2 torr does the Lorentzian shape function account for the detailed structure of the pressure-broadened water vapor line, but down to 0.1 torr the half-power point (peak dispersion) remains pressure proportional.

Acknowledgement—The authors wish to thank M. J. VETTER who designed and constructed the bimodal cavity and the electronic circuitry, and M. S. JOHNSON who helped to set up the experiment.

REFERENCES

1. H. J. LIEBE, M. J. VETTER and M. C. THOMPSON, JR. (to be published).
2. J. H. JAFFEE, In *Advances in Spectroscopy* (Edited by H. W. THOMPSON), Vol. II, Interscience Publishers, New York (1961).

3. H. W. DeWijn, P. J. Severin and K. van der Veen, *Physica* **27,** 1146 (1961).
4. M. J. Vetter and M. C. Thompson, Jr., *Rev. Sci. Instrum.* **38,** 1826 (1967).
5. H. J. Liebe, *Nachr. Tech. Z.* NTZ **18,** 510 (1965).
6. M. C. Thompson, Jr. and M. J. Vetter, *Rev. Sci. Instrum.*, **39,** 1333 (1968).
7. S. A. Zhevakin and A. P. Naumov, *Radio Eng. and Electr. Phys.* (*Engl. Transl.*) **12,** 1067 (1967).
8. C. H. Townes and F. R. Merritt, *Phys. Rev.* **70,** 558 (1946).
9. J. Gilbert and R. M. Vaillan Court, *Proc. IEEE* **54,** 514 (1966) and private communication.
10. G. Oakson, *Transient Effect Spectrometer for K-Band Water Line Emission*, Canadian Armament Res. Develop. Establ., Valcartier Quebec, Report No. 046-95-10-24 (1966).
11. G. Becker and S. Autler, *Phys. Rev.* **70,** 300 (1946).
12. J. R. Rusk, *J. Chem. Phys.* **42,** 493 (1963).
13. L. Frenkel and D. Woods, *Proc. IEEE* **54,** 498 (1966).
14. R. B. Sanderson and N. Ginsburg, *JQSRT* **3,** 435 (1963).
15. W. S. Benedict and L. D. Kaplan, *JQSRT* **4,** 453 (1964).
16. B. West and M. Mizushima, *Table of Rotational Transition Strengths for Asymmetric Rotors*, Contract No. DA-36-039-SC-87277, University of Colorado, Boulder, Colorado (1961).
17. R. H. Schwendeman and V. W. Laurie, *Tables of Line Strengths*. Pergamon Press, Oxford (1956).
18. E. Hiedemann and R. D. Spence, *Z. f. Physik* **133,** 109 (1952).
19. H. J. Liebe, *Nachr. Tech. Z.*, NTZ **19,** 79 (1966).
20. G. Birnbaum, Microwave Pressure Broadening, in *Advances in Chemical Physics* (Edited by J. O. Hirschfelder), vol. XII. Interscience Publishers, New York (1967).
21. W. S. Benedict, H. H. Claasen and J. H. Shaw, *J. Res. NBS* **49,** 91 (1952).
22. D. L. Dobbins and A. H. LaGrone, *Vibrational and Rotational Energy Levels of Water Vapor*, Report No. P21 of the University of Texas, Austin (1967).
23. M. Lichtenstein, V. E. Derr and J. J. Gallagher, *J. Molec. Spectrosc.* **20,** 391 (1966).
24. M. Mizushima, *Progr. Theor. Phys.* Suppl. No. 40, 207 (1967).
25. K. Matsuura, Y. Suguira and G. M. Hatoyama, *J. Phys. Soc. Japan* **12,** 314 (1957).
26. G. Schulten, *Frequenz* **20,** 10 (1966).
27. H. J. Liebe and T. A. Dillon, *J. Chem. Phys.*, in press.
28. J. E. Chamberlain, *JQSRT* **7,** 151 (1967).